Experimental Study of $\langle 110 \rangle$ Uniaxial Stress Effects on p-Channel GaAs Quantum-Well FETs

Ling Xia, *Student Member, IEEE*, Vadim Tokranov, Serge R. Oktyabrsky, *Senior Member, IEEE*, and Jesús A. del Alamo, *Fellow, IEEE*

***Abstract*—The impact of $\langle 110 \rangle$ uniaxial stress on 2-D hole gas (2DHG) transport and charge control in a GaAs quantum well (QW) is studied through wafer bending experiments. Ungated Hall bars and QW field-effect transistors (FETs) were characterized under various stress levels. Through Hall measurements, changes in hole mobility and concentration due to applied stress were separated. The piezoresistance coefficients of the 2DHG along the two $\langle 110 \rangle$ directions in the GaAs QW have been determined for the first time. We found that the linear-regime current of the QW-FET changes due to a combination of piezoelectric effect and hole mobility changes. The value of these coefficients suggests that uniaxial strain engineering is a viable technique to improve p-channel GaAs QW-FET performance for future logic applications.**

***Index Terms*—GaAs, Hall measurement, piezoresistance coefficient, quantum-well field-effect transistor (QW-FET), uniaxial stress, 2-D hole gas (2DHG).**

I. INTRODUCTION

IN RECENT times, InGaAs field-effect transistors (FETs) have attracted significant attention for applications in future logic technology [1]. n-Channel InGaAs quantum-well (QW) FETs showed over 2× electron injection velocity compared with Si at a reduced voltage [2]. This high injection velocity is critical for scaling devices beyond the 15-nm technology node, as it compensates continuously increasing parasitic capacitance that comes with device scaling [3].

To implement complementary logic circuits based on InGaAs, p-channel FETs based on arsenides are ideal in terms of process integration. However, hole mobility in arsenides is only comparable with that in Si [4], whereas other candidate p-channel materials such as Ge [5] and, more recently, InGaSb alloys [6], [7] possess higher hole mobility than that of conventional Si.

A technological approach to enhance pFET performance is the introduction of uniaxial strain. As early as in 1962, Hensel and Feher experimentally found that strain lifts valence-band degeneracy and changes hole effective masses in Si [8]. These effects inspired the demonstration in 1993 of the first strained Si p-channel metal–oxide–semiconductor field-effect transistor (pMOSFET) with enhanced hole mobility [9]. After a decade of effort, strain engineering was incorporated into a commercial Si complementary metal–oxide–semiconductor at the 90-nm technology node [10]. In fact, the introduction of uniaxial strain has enhanced the pMOSFET performance so much that the traditional advantage of the n-channel MOSFET has been almost completely erased at the 32-nm node [11]. In particular, $\langle 110 \rangle$ compressive stress has been found to be most effective in p-channel device enhancement. Up to 200% enhancement in mobility has been demonstrated in uniaxially compressively strained Si pMOSFETs [12], [13]. On other materials, for example, Ge, uniaxial strain effects have been also explored to enhance pFET performance [14].

Employing strain effects to enhance pFET performance in arsenides was theoretically suggested to be feasible in a review article by O'Reilly [15]. On the experiment side, past efforts in strain-engineered arsenides to modify hole transport were devoted to introducing biaxial strain into the channel through the pseudomorphic growth of lattice-mismatched InGaAs [4], [16]. In $\mathrm{In}_x\mathrm{Ga}_{1-x}\mathrm{As}$, the highest hole mobility reported to date is 400 $\mathrm{cm}^2/\mathrm{V}\cdot\mathrm{s}$ in $\mathrm{In}_{0.82}\mathrm{Ga}_{0.18}\mathrm{As}$ with a 2% biaxial compressive strain level on an InP substrate [4].

In contrast, uniaxial stress has not been explored for hole mobility improvement in arsenide-based devices. This paper reports an experimental study of the effect of uniaxial stress on 2-D hole gas (2DHG) transport and electrostatics in modulation-doped GaAs QWs. Electrical characteristics of FETs and Hall bars were measured under various levels of $\langle 110 \rangle$ stress externally applied to the devices. The carrier concentration and mobility were found to change as a result of strain. We found that this is due to a combination of piezoelectric effect, valence-band changes, and, possibly, modification in scattering rates. The longitudinal and transverse $\langle 110 \rangle$ piezoresistance coefficients that capture the change in hole mobility due to the uniaxial stress of the 2DHG in the GaAs QW have been determined for the first time.

II. EXPERIMENTAL

A. Device Fabrication

The devices used in this paper are FETs and ungated Hall bars fabricated on an AlGaAs/GaAs modulation-doped QW

Manuscript received March 29, 2011; revised May 6, 2011; accepted May 10, 2011. Date of publication June 27, 2011; date of current version July 22, 2011. This work was supported by the Focus Center Research Program–Materials, Structures and Devices Focus Center (FCRP-MSD) and Intel Corporation. The review of this paper was arranged by Editor G. Ghione.

L. Xia and J. A. del Alamo are with the Microsystems Technology Laboratories, Massachusetts Institute of Technology, Cambridge, MA 02139 USA (e-mail: lingxia@mit.edu).

V. Tokranov and S. R. Oktyabrsky are with the University at Albany, State University of New York, Albany, NY 12222 USA.

Color versions of one or more of the figures in this paper are available online at http://ieeexplore.ieee.org.

Digital Object Identifier 10.1109/TED.2011.2157696

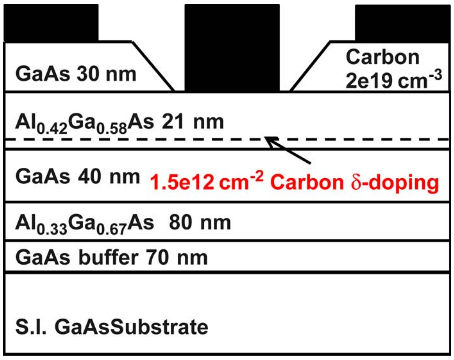

Fig. 1. Cross section of fabricated GaAs QW-FETs.

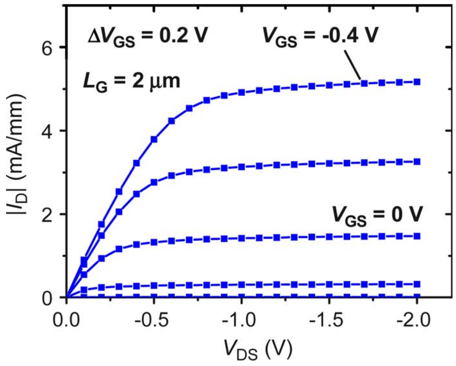

Fig. 2. Typical output characteristics of a QW-FET with $L_G = 2\ \mu$m.

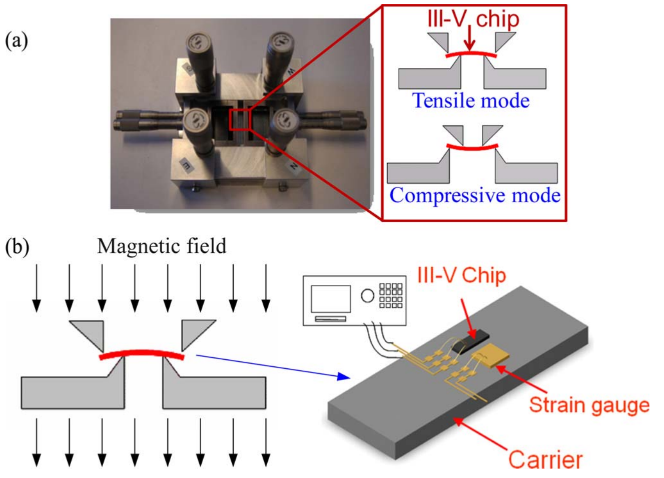

Fig. 3. (a) Chip-bending apparatus and its working mechanism to introduce uniaxial stress to III–V chips. (b) Configuration of a magnetic field and electrical connections to the mounted chips.

heterostructure grown by molecular-beam epitaxy (see Fig. 1). The heterostructure exhibits hole mobility μ_h of 277 $\mathrm{cm}^2/\mathrm{V}\cdot\mathrm{s}$ with a sheet hole density of $6 \times 10^{11}\ \mathrm{cm}^{-2}$, as measured from the fabricated Hall bars.

The fabrication process starts with mesa etching by a $H_3PO_4/H_2O_2/H_2O$ (1:1:25) solution. After this, ohmic contacts were formed by electron-beam-evaporated Ni/Au/Zn/Au (10 nm/10 nm/30 nm/200 nm) and rapid thermal annealing at 440 °C for 30 s. Following this, gate recess for the FETs was performed by a citric acid/H_2O_2 (4:1) solution [17]. The GaAs cap layer was selectively etched. Ti/Pt/Au (20 nm/20 nm/200 nm) was evaporated to form the gate. The ungated Hall bars were recessed at the same time but were covered during gate metal evaporation. Finally, Ti/Au (20 nm/200 nm) was evaporated to form contact pads.

The QW-FETs have a gate length L_G of 2 μm and a gate width of 50 μm. The ungated Hall bars are 20-μm wide and 300-μm long. The cross section and output characteristics of a finished QW-FET are shown in Figs. 1 and 2.

B. Chip-Bending Setup

Uniaxial stress was introduced to the samples through a chip-bending apparatus in Fig. 3(a). The apparatus is able to perform four-point bending upon chips positioned between two pairs of jaws [see Fig. 3(a)]. Either tensile or compressive stress can be applied depending on the configuration of the jaws.

Our experimental methodology has been optimized to apply large strain to III–V chips. This was accomplished by thinning the chips to ∼120 μm, by mechanical grinding, and by attaching them to an aluminum carrier. This way, we were able to introduce a strain level of ±0.3% to GaAs chips before they crack. This is about 5× the value that can be attained otherwise. We verified that loading and unloading of strain have no hysteretic behavior. The level of strain in the experiments that follow was kept below one third of the maximum strain in order to secure the samples for repeated measurements.

The strain level at the chip surface was calibrated by surface deflection (Tencor Flexus 2320) and strain gauge measurements. Strain transfer from the Al carrier to the mounted GaAs chip was checked by comparing the readings of two strain gauges, i.e., one on the Al surface and the other one on the GaAs chip surface. The difference between these two readings is within 3.5%.

As illustrated in Fig. 3(b), the devices were wire bonded to metal pads attached to the Al carrier. The pads and the Al carrier were insulated by a plastic film. The metal pads were then connected to a semiconductor parameter analyzer. The transfer characteristics of the FETs were measured at a drain-to-source voltage V_{DS} of -50 mV, which is low enough to avoid heating effects and significant parasitic ohmic drops. Hall measurements were conducted with a pair of permanent magnets, which apply a magnetic field $(B = 3470\ \mathrm{G})$ perpendicular to the sample surface. The major body of the apparatus is made of aluminum and demagnetized stainless steel. Therefore, the mechanical parts around the semiconductor samples do not affect the distribution of the magnetic field. Measurements with the magnetic field pointing up and down were conducted at each stress level.

The directions of applied stress and devices require some elaboration. On the same substrate, we have ungated Hall bars and FETs with transport directions aligned with the two cleaving crystallographic directions on the (100) surface ([110] and [$-$110]). We applied uniaxial stress along these two orthogonal $\langle 110 \rangle$ directions in order. All the Hall bars and FETs were measured under each stress condition. The directions of hole transport and stress are shown in Fig. 4. To track the relation, the stress is named with the following two subscripts: The first

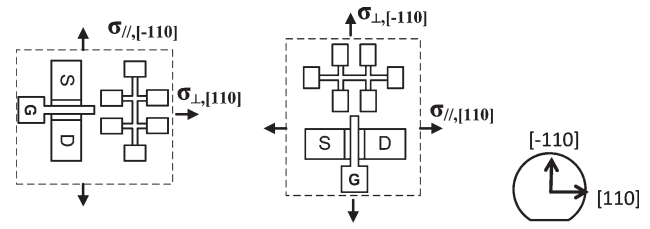

Fig. 4. Schematic of the directions of test structures and applied stress and notation used for stress. The wafer crystallographic directions are indicated on the right.

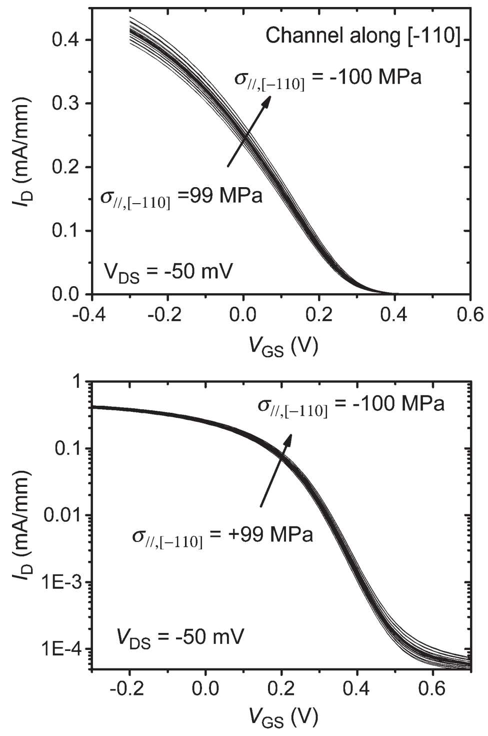

Fig. 5. Transfer characteristics in (top) a linear scale and (bottom) a semilogarithmic scale of a GaAs QW-FET as a function of [−110] uniaxial stress. Both channel and stress are aligned with the [−110] crystalline direction.

one indicates the relative direction between stress and device current flow (parallel or perpendicular), and the second one indicates the absolute crystallographic direction of the stress ([110] or [−110]).

III. RESULTS AND DISCUSSION

Fig. 5 shows a representative example of the shift of the transfer characteristics of a p-channel GaAs QW-FET under uniaxial stress. In this particular example, the stress is along [−110] and parallel to the channel direction. Linear-regime drain current I_{Dlin} measured with $V_{DS} = 50$ mV and $V_{GS} = -0.3$ V increased by 10.4% as $\sigma_{//,[-110]}$ changes from tensile 99 MPa to compressive 100 MPa. Threshold voltage V_T is also shown to be affected by the applied strain.

Extracting the hole mobility change from the change in I_{Dlin} is not straightforward. Our previous study [18], [19] showed that ⟨110⟩ uniaxial stress changes the 2-D electron concentration in an n-channel III–V QW-FET structure through the piezoelectric effect by shifting threshold voltage V_T and gate capacitance C_G. Therefore, ΔI_{Dlin} in the present devices likely consists of not only a change in μ_h but also a change in 2DHG concentration p_s. A commonly used method to extract C_G and p_s in MOSFETs is through C–V measurements. However, in our QW-FETs, the gate leakage current is substantial and prevents accurate C–V measurements.

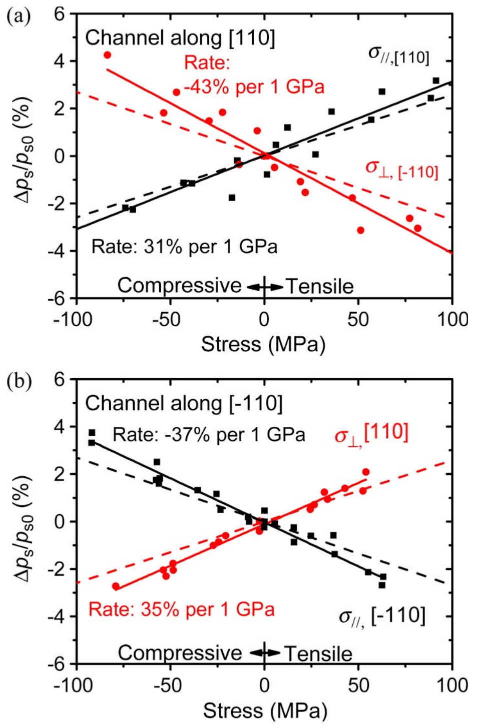

Fig. 6. (Symbols) Normalized change in sheet hole concentration p_s as a function of ⟨110⟩ stress. Results from ungated Hall bars along (a) [110] and (b) [−110]. (Solid lines) Linear fittings to the data. (Dashed lines) Δp_s predicted by the Schrodinger–Poisson simulations.

In this paper, Hall measurements were used to separate the changes in μ_h and p_s. Fig. 6 summarizes the measured relative change in p_s with ⟨110⟩ uniaxial stress (symbols). Here, we found that Δp_s almost solely depends on the absolute alignment between stress and crystallographic direction. The directions of transport in the Hall bar have rather little effect on Δp_s, as observed if we compare Fig. 6(a) and (b). This behavior of Δp_s suggests that the piezoelectric effect dominates the change in p_s, which is similar to the situation in [18] and [19]. In fact, by incorporating the piezoelectric effect into a 1-D Schrodinger–Poisson simulator, Δp_s can be well predicted, as shown by the dashed lines in Fig. 6. The piezoelectric coefficients used in the simulations are $e_{14}(\mathrm{GaAs}) = -0.16\ \mathrm{C/cm}^2$ [20] and $e_{14}(\mathrm{AlAs}) = -0.25\ \mathrm{C/cm}^2$. This $e_{14}(\mathrm{AlAs})$ was adjusted to be slightly larger than $-0.225\ \mathrm{C/cm}^2$ given in [20]. This mild adjustment leads to simulation results that provide a better match to both Δp_s and ΔV_T (discussed below). A similar $e_{14}(\mathrm{AlAs})$ value was experimentally deduced in [21]. The value of e_{14} for $\mathrm{Al_{0.42}Ga_{0.58}As}$ was linearly interpolated from $e_{14}(\mathrm{GaAs})$ and $e_{14}(\mathrm{AlAs})$.

The impact of stress on μ_h measured from Hall measurements is shown in Fig. 7. $\Delta\mu_h$ also changes with stress in an anisotropic way. However, unlike for Δp_s, the direction of the

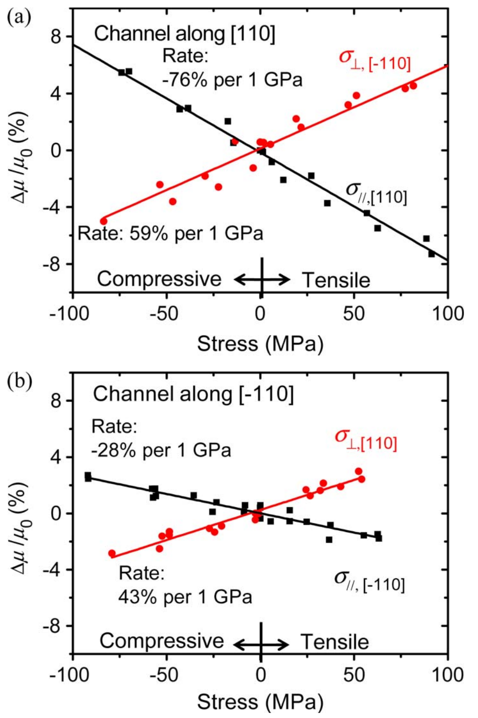

Fig. 7. Normalized change in hole mobility as a function of $\langle 110\rangle$ stress. Results from Hall bars along (a) [110] and (b) [−110]. (Solid lines) Linear fittings to the data.

Hall bar determines the sign of $\Delta\mu_h$. In particular, μ_h increases with compressive $\sigma_{//}$ and tensile $\sigma_\perp$, whereas it decreases with tensile $\sigma_{//}$ and compressive $\sigma_\perp$. This effect is due to the impact of stress on the valence-band dispersion relation and, therefore, hole transport. Similar effects have been widely observed in Si and Ge [22].

In addition to the valence-band change, the aforementioned change in p_s may be also affecting μ_h. As shown in Fig. 7, the slopes of $\Delta\mu_h$ versus stress with the same relative stress directions are quite different, i.e., the crystalline directions affect the sensitivity of μ_h to uniaxial stress. This effect is likely due to the dependence of μ_h on p_s. As discussed in [23] and [24], an increase/decrease in p_s can lead to a decrease/increase in μ_h. This has been also shown in separate experiments by other authors [25]. A change in p_s enhances the sensitivity of μ_h to stress ($//$ or $\perp$) when the channel is along [110], whereas it weakens the sensitivity when the channel is aligned to [−110]. This is the reason why the apparent sensitivities of μ_h to either $\sigma_{//}$ or $\sigma_\perp$ are different when the channel is aligned to the different crystalline directions.

To extract the dependence of μ_h on applied stress, excluding the change in μ_h due to Δp_s, we note that

$$d\mu = \left.\frac{\partial\mu}{\partial\sigma}\right|_{p_s} d\sigma + \left.\frac{\partial\mu}{\partial p_s}\right|_{\sigma} dp_s = \left.\frac{\partial\mu}{\partial\sigma}\right|_{p_s} d\sigma + \left.\frac{\partial\mu}{\partial p_s}\right|_{\sigma} \frac{dp_s}{d\sigma} d\sigma. \tag{1}$$

Therefore

$$\frac{d\mu}{d\sigma} = \left.\frac{\partial\mu}{\partial\sigma}\right|_{p_s} + \left.\frac{\partial\mu}{\partial p_s}\right|_{\sigma} \frac{dp_s}{d\sigma}. \tag{2}$$

Following the expected power-law dependence of μ on p_s in [23], let us assume that

$$\mu_{//} \propto p_s^{\alpha_{//}} \tag{3}$$

$$\mu_\perp \propto p_s^{\alpha_\perp}. \tag{4}$$

As the change in p_s in our experiments is very small, employing constant power indices α is appropriate. Assuming two α constants for parallel and perpendicular directions, respectively, means that the dependence of μ_h on p_s is determined by the relation ($//$ or $\perp$) between the directions of μ_h and stress σ but is insensitive to the crystalline direction of σ ([110] or [−110]). The underlying physics is that the responses of valence-band dispersion are asymmetric to $\sigma_{//}$ and $\sigma_\perp$, but this asymmetry is not affected by the crystalline direction of stress. This assumption has been verified by $k\cdot p$ simulations of valence-band dispersion in the studied QW with the piezoelectric effect included. Values of α between 0 and -1, depending on the hole concentration, are commonly shown [23], [24].

Traditionally, piezoresistance coefficient π has been used to represent the relative change in resistivity with respect to applied stress [26], i.e., $\pi = \Delta\rho/(\rho\cdot\sigma)$, where ρ is the resistivity. In studies of strain effects on FETs, π was extracted from the change in mobility in FETs with respect to applied stress under a constant carrier density [27], [28]. To allow direct comparisons between FETs based on GaAs and other materials, we adapt the latter definition, which is formalized as

$$\pi = -\left.\frac{\partial\mu}{\partial\sigma}\right|_{p_s} \cdot \frac{1}{\mu_0}. \tag{5}$$

By inserting (3)–(5) into (2), we can obtain a set of four equations for stress with various combinations of relative and crystalline directions, i.e.,

$$\frac{d\ln\mu_{[110]}}{d\sigma_{//,[110]}} = -\pi_{//} + \alpha_{//}\cdot\frac{d\ln p_s}{d\sigma_{//,[110]}} \tag{6}$$

$$\frac{d\ln\mu_{[-110]}}{d\sigma_{//,[-110]}} = -\pi_{//} + \alpha_{//}\cdot\frac{d\ln p_s}{d\sigma_{//,[-110]}} \tag{7}$$

$$\frac{d\ln\mu_{[-110]}}{d\sigma_{\perp,[110]}} = -\pi_\perp + \alpha_\perp\cdot\frac{d\ln p_s}{d\sigma_{\perp,[110]}} \tag{8}$$

$$\frac{d\ln\mu_{[110]}}{d\sigma_{\perp,[-110]}} = -\pi_\perp + \alpha_\perp\cdot\frac{d\ln p_s}{d\sigma_{\perp,[-110]}}. \tag{9}$$

The values of $d\ln p_s/d\sigma$ and $d\ln\mu/d\sigma$ can be obtained in Figs. 6 and 7, respectively. Therefore, solving (6) and (7) yields $\pi_{//}$ and $\alpha_{//}$, whereas $\pi_\perp$ and $\alpha_\perp$ can be obtained in (8) and (9). Following this procedure, we obtain piezoresistance coefficients $\pi_{//} = 54\ \text{cm}^2/\text{dyn}$ and $\pi_\perp = -50\ \text{cm}^2/\text{dyn}$. $\alpha_{//}$ and $\alpha_\perp$ are extracted to be -0.7 and -0.2.

IV. DISCUSSION

Fig. 8 compares the piezoresistance coefficients experimentally determined in pFETs and bulk p-type Si, Ge, and GaAs [27]–[30]. It can be shown that the $\pi_{//}$ of the GaAs 2DHG is 3× the bulk GaAs value. Furthermore, GaAs 2DHG $\pi_{//}$ is

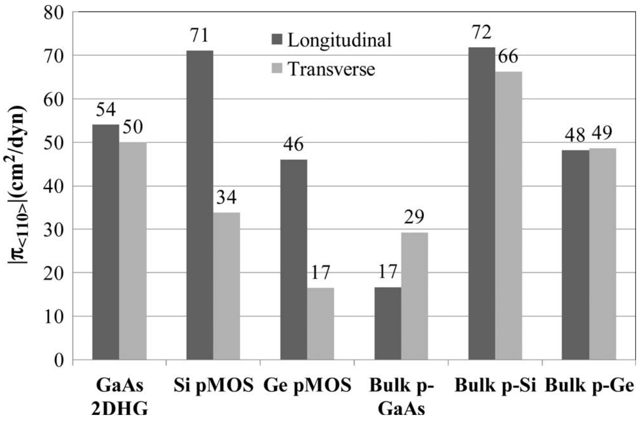

Fig. 8. Comparison between the p-type piezoresistance coefficients of GaAs, Si, and Ge. Both bulk and FET results are shown. In all situations, the sign of longitudinal coefficients $\pi_{//}$ is positive, whereas the sign of transverse coefficients $\pi_{\perp}$ is negative.

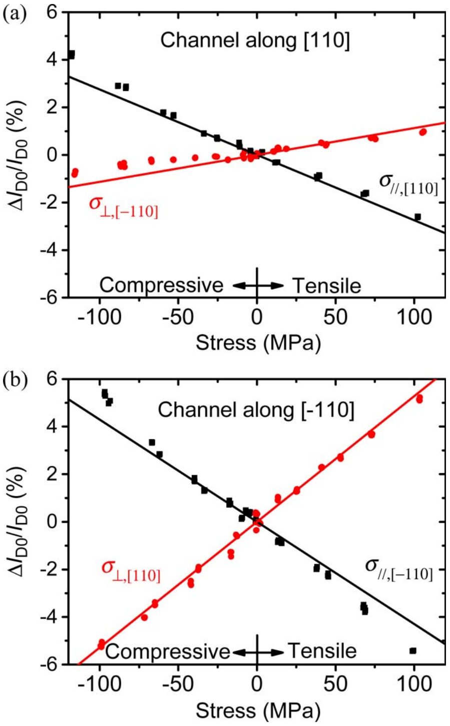

Fig. 9. (Symbols) Normalized change in linear-regime drain current as a function of applied ⟨110⟩ uniaxial stress. The channel direction is along (a) [110] and (b) [−110]. (Solid lines) Estimations of $-\Delta R_{\mathrm{tot}}/R_{\mathrm{tot0}}$ that include both fixed parasitic resistances and $-\Delta R_{\mathrm{sh}}/R_{\mathrm{sh0}}$ measured in ungated Hall bars.

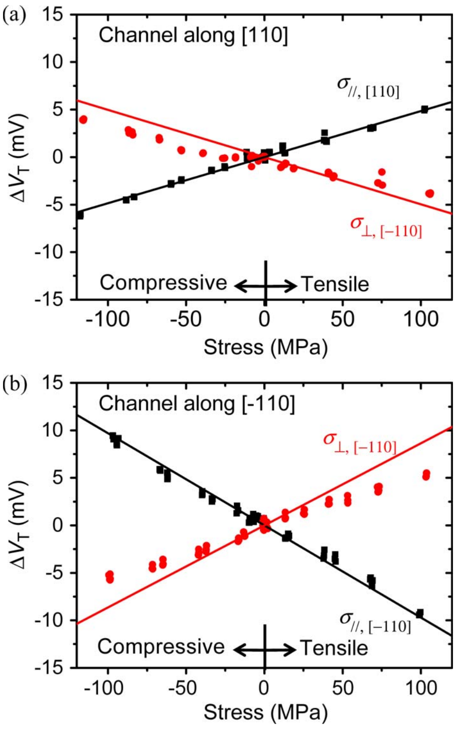

Fig. 10. Change in threshold voltage as a function of stress. (Symbols) Results from the QW-FET along (a) [110] and (b) [−110]. (Solid lines) ΔV_T predicted by a model that includes V_T shifts due to the electrostatic and mobility changes induced by strain.

17% higher than the Ge pMOSFET value. These facts suggest that the introduction of uniaxial strain to GaAs QW-FETs can improve the device performance in a significant way.

Interestingly, the Δp_s and $\Delta \mu_h$ measured from Hall measurements are consistent with the changes observed in QW-FET characteristics. We chose the normalized change in I_{Dlin} at $V_{GS} = 0$ V $(\Delta I_{D0}/I_{D0})$ and ΔV_T extracted at $I_D =$ 0.05 mA/mm as the two figures of merit of QW-FETs. Fig. 9 summarizes the measured $\Delta I_{D0}/I_{D0}$ in two orthogonal GaAs QW-FETs as a result of uniaxial stress application (symbols). $\Delta I_{D0}/I_{D0}$ essentially reflects the change in the total resistance of the FETs $(\Delta R_{\mathrm{tot}}/R_{\mathrm{tot0}})$. Similar to the case in [31], $R_{\mathrm{tot0}} = R_{\mathrm{sh0}} \cdot L_G/W_G + R_p$, where R_p is a fixed parasitic resistance. Considering both the change in sheet resistance $(\Delta R_{\mathrm{sh}}/R_{\mathrm{sh0}})$ measured from the ungated Hall bars and R_p obtained by the transmission line method, we found that $\Delta I_{D0}/I_{D0}$ follows well the expected $-\Delta R_{\mathrm{tot}}/R_{\mathrm{tot0}}$ of the FETs, as shown in Fig. 9.

Changes in QW-FET V_T can be also well explained by Δp_s and $\Delta \mu_h$. The apparent ΔV_T measured at a constant subthreshold current is the sum of two components [31], i.e.,

$$\Delta V_T^{\mathrm{app}} = \Delta V_T^{\mathrm{elec}} + \frac{nkT}{q} \ln\left(1 + \frac{\Delta \mu_h}{\mu_h}\right) \tag{10}$$

where n is the ideality factor, k is the Boltzmann's constant, and T is the temperature.

On the right-hand side of (10), the first term $\Delta V_T^{\mathrm{elec}}$ is due to the change of valence-band bending induced by the piezoelectric effect. $\Delta V_T^{\mathrm{elec}}$ was extracted as the shift of V_{GS} for a constant p_s $(10^{11}\ \mathrm{cm^{-2}})$ from the 1-D Schrodinger–Poisson simulations under various stress conditions. This group of simulations is the same group that led to the $\Delta p_s/p_{s0}$ values in Fig. 6. The second term on the right-hand side of (10) is due to the shift of the subthreshold drain current induced by a hole mobility shift. Ideality factor n was extracted from the subthreshold slope at $V_{GS} = V_T$ in the measured transfer characteristics. $\Delta \mu_h/\mu_h$ is from the Hall measurement data in Fig. 7. As shown in Fig. 10, the measured ΔV_T in the QW-FET with applied ⟨110⟩ stress (symbols) agrees well with the overall ΔV_T calculated using (10) (solid lines). The excellent agreement among measurements in FETs and Hall bars, as well as simulations, gives great credibility to our extraction methodology and our identification of the relevant physics.

V. CONCLUSION

This paper has experimentally studied the impact of $\langle 110\rangle$ uniaxial stress on transport in a GaAs 2DHG. The hole mobility and concentration are found to change at the same time due to strain. The underlying mechanisms include the strain-induced transport change and the piezoelectric effect. The effect of mobility change was extracted from Hall measurements. For the first time, the $\langle 110\rangle$ piezoresistance coefficients of the GaAs 2DHG with a hole density of 6×10^{11} cm^{-2} has been determined. The values are $\pi_{/\!/} = 54$ cm^2/dyn and $\pi_\perp = -50$ cm^2/dyn. The changes in μ_h and p_s manifest themselves as changes in I_{Dlin} and V_T in QW-FETs. Compared with values in Si and Ge pMOSFETs, the piezoresistance coefficients of the GaAs 2DHG suggest that uniaxial strain engineering is expected to benefit the GaAs QW-FET significantly.

ACKNOWLEDGMENT

Device fabrication was performed at the Microsystems Technology Laboratories, Massachusetts Institute of Technology. Wafer epitaxy was done at the University at Albany, State University of New York.

REFERENCES

[1] D.-H. Kim and J. A. del Alamo, "30 nm E-mode InAs PHEMTs for THz and future logic applications," in *IEDM Tech. Dig.*, 2008, pp. 719–722.

[2] D.-H. Kim and J. A. del Alamo, "Extraction of virtual-source injection velocity in sub-100 nm III–V HFETs," in *IEDM Tech. Dig.*, 2009, pp. 861–864.

[3] A. Khakifirooz and D. A. Antoniadis, "MOSFET performance scaling—Part I: Historical trends," *IEEE Trans. Electron Devices*, vol. 55, no. 6, pp. 1391–1400, Jun. 2008.

[4] A. Mesquida Kusters, A. Kohl, K. Heime, T. Schapers, D. Uhlisch, B. Lengeler, and H. Lüth, "Low- and high-field transport properties of pseudomorphic In$_x$Ga$_{1-x}$As/InP $(0.73 < x < 0.82)$ p-type modulation-doped single-quantum-well structures," *J. Appl. Phys.*, vol. 75, no. 7, pp. 3507–3515, Apr. 1994.

[5] P. Zimmerman, G. Nicholas, B. De Jaeger, B. Kaczer, A. Stesmans, L. A. Ragnarsson, D. P. Brunco, F. E. Leys, M. Caymax, G. Winderickx, K. Opsomer, M. Meuris, and M. M. Heyns, "High performance Ge pMOS devices using a Si-compatible process flow," in *IEDM Tech. Dig.*, 2006, pp. 1–4.

[6] B. R. Bennett, M. G. Ancona, J. B. Boos, and B. V. Shanabrook, "Mobility enhancement in strained p-InGaSb quantum wells," *Appl. Phys. Lett.*, vol. 91, no. 4, p. 042 104, Jul. 2007.

[7] M. Radosavljevic, T. Ashley, A. Andreev, S. D. Coomber, G. Dewey, M. T. Emeny, M. Fearn, D. G. Hayes, K. P. Hilton, M. K. Hudait, R. Jefferies, T. Martin, R. Pillarisetty, W. Rachmady, T. Rakshit, S. J. Smith, M. J. Uren, D. J. Wallis, P. J. Wilding, and R. Chau, "High-performance 40 nm gate length InSb p-channel compressively strained quantum well field effect transistors for low-power ($V_{\mathrm{CC}} = 0.5$ V) logic applications," in *IEDM Tech. Dig.*, 2008, pp. 727–730.

[8] J. C. Hensel and G. Feher, "Cyclotron resonance experiments in uniaxially stressed silicon: Valence band inverse mass parameters and deformation potentials," *Phys. Rev.*, vol. 129, no. 3, pp. 1041–1062, Feb. 1963.

[9] D. K. Nayak, J. C. S. Woo, J. S. Park, K. L. Wang, and K. P. MacWilliams, "High-mobility p-channel metal–oxide–semiconductor field-effect transistor on strained Si," *Appl. Phys. Lett.*, vol. 62, no. 22, pp. 2853–2855, May 1993.

[10] K. Mistry, M. Armstrong, C. Auth, S. Cea, T. Coan, T. Ghani, T. Hoffmann, A. Murthy, J. Sandford, R. Shaheed, K. Zawadzki, K. Zhang, S. Thompson, and M. Bohr, "Delaying forever: Uniaxial strained silicon transistors in a 90 nm CMOS technology," in *VLSI Symp. Tech. Dig.*, 2004, pp. 50–51.

[11] S. Natarajan, M. Armstrong, M. Bost, R. Brain, M. Brazier, C. H. Chang, V. Chikarmane, M. Childs, H. Deshpande, K. Dev, G. Ding, T. Ghani, O. Golonzka, W. Han, J. He, R. Heussner, R. James, I. Jin, C. Kenyon, S. Klopcic, S.-H. Lee, M. Liu, S. Lodha, B. McFadden, A. Murthy, L. Neiberg, J. Neirynck, P. Packan, S. Pae, C. Parker, C. Pelto, L. Pipes, J. Sebastian, J. Seiple, B. Sell, S. Sivakumar, B. Song, K. Tone, T. Troeger, C. Weber, M. Yang, A. Yeoh, and K. Zhang, "A 32 nm logic technology featuring 2nd-generation high-$\kappa +$ metal-gate transistors, enhanced channel strain and 0.171 $\mu\mathrm{m}_2$ SRAM cell size in a 291 Mb array," in *IEDM Tech. Dig.*, 2008, pp. 941–943.

[12] L. Washington, F. Nouri, S. Thirupapuliyur, G. Eneman, P. Verheyen, V. Moroz, L. Smith, X. Xu, M. Kawaguchi, T. Huang, K. Ahmed, M. Balseanu, L.-Q. Xia, M. Shen, Y. Kim, R. Rooyackers, K. De Meyer, and R. Schreutelkamp, "pMOSFET with 200% mobility enhancement induced by multiple stressors," *IEEE Electron Device Lett.*, vol. 27, no. 6, pp. 511–513, Jun. 2006.

[13] S. K. H. Fung, H. C. Lo, C. F. Cheng, W. Y. Lu, K. C. Wu, K. H. Chen, D. H. Lee, Y. H. Liu, I. L. Wu, C. T. Li, C. H. Wu, F. L. Hsiao, T. L. Chen, W. Y. Lien, C. H. Huang, P. W. Wang, Y. H. Chiu, L. T. Lin, K. Y. Chen, H. J. Tao, H. C. Tuan, Y. J. Mii, and Y. C. Sun, "45 nm SOI CMOS Technology with 3 × hole mobility enhancement and asymmetric transistor for high performance CPU application," in *IEDM Tech. Dig.*, 2007, pp. 1035–1037.

[14] L. Gomez, C. Ni Chléirigh, P. Hashemi, and J. L. Hoyt, "Enhanced hole mobility in high Ge content asymmetrically strained-SiGe p-MOSFETs," *IEEE Electron Device Lett.*, vol. 31, no. 8, pp. 782–784, Aug. 2010.

[15] E. P. O'Reilly, "Valence band engineering in strained-layer structures," *Semicond. Sci. Technol.*, vol. 4, no. 3, pp. 121–137, Mar. 1989.

[16] R. A. Kiehl, H. Shtrikman, and J. Yates, "Parallel and perpendicular hole transport in heterostructures with high AlAs mole-fraction barriers," *Appl. Phys. Lett.*, vol. 58, no. 9, pp. 954–956, Mar. 1991.

[17] C. D. Gregory, F. T. Wen, and C. James, "Etch rates and selectivities of citric acid/hydrogen peroxide on GaAs, Al$_{0.3}$Ga$_{0.7}$As, In$_{0.2}$Ga$_{0.8}$As, In$_{0.53}$Ga$_{0.47}$As, In$_{0.52}$Al$_{0.48}$As, and InP," *J. Electrochem. Soc.*, vol. 139, no. 3, pp. 831–835, Mar. 1992.

[18] L. Xia and J. A. del Alamo, "Impact of $\langle 110\rangle$ uniaxial strain on n-channel In$_{0.15}$Ga$_{0.85}$As high electron mobility transistors," *Appl. Phys. Lett.*, vol. 95, no. 24, p. 243 504, 2009.

[19] L. Xia and J. A. del Alamo, "Erratum: "Impact of <110> uniaxial strain on n-channel In$_{0.15}$Ga$_{0.85}$As high electron mobility transistors" [Appl. Phys. Lett. 95, 243504 (2009)]," *Appl. Phys. Lett.*, vol. 97, no. 2, p. 029 901, Jul. 2010.

[20] S. Adachi, "GaAs, AlAs, and Al$_x$Ga$_{1-x}$As: Material parameters for use in research and device applications," *J. Appl. Phys.*, vol. 58, no. 3, pp. R1–R29, Aug. 1985.

[21] Y. Liu, Z. L. Rang, A. K. Fung, C. Cai, P. P. Ruden, M. I. Nathan, and H. Shtrikman, "Uniaxial-stress dependence of Hall effect in an AlGaAs/GaAs modulation-doped heterojunction," *Appl. Phys. Lett.*, vol. 79, no. 27, pp. 4586–4588, Dec. 2001.

[22] M. L. Lee, E. A. Fitzgerald, M. T. Bulsara, M. T. Currie, and A. Lochtefeld, "Strained Si, SiGe, and Ge channels for high-mobility metal–oxide–semiconductor field-effect transistors," *J. Appl. Phys.*, vol. 97, no. 1, p. 011 101, Jan. 2005.

[23] M. V. Fischetti, Z. Ren, P. M. Solomon, M. Yang, and K. Rim, "Six-band $k \cdot p$ calculation of the hole mobility in silicon inversion layers: Dependence on surface orientation, strain, and silicon thickness," *J. Appl. Phys.*, vol. 94, no. 2, pp. 1079–1095, Jul. 2003.

[24] Y. Zhang, M. V. Fischetti, B. Sorée, and T. O'Regan, "Theory of hole mobility in strained Ge and III–V p-channel inversion layers with high-k insulators," *J. Appl. Phys.*, vol. 108, no. 12, p. 123 713, Dec. 2010.

[25] M. Kudo, H. Matsumoto, T. Tanimoto, T. Mishima, and I. Ohbu, "Improved hole transport properties of highly strained In$_{0.35}$Ga$_{0.65}$As channel double-modulation-doped structures grown by MBE on GaAs," *J. Cryst. Growth*, vol. 175/176, pp. 910–914, May 1997.

[26] C. S. Smith, "Piezoresistance effect in germanium and silicon," *Phys. Rev.*, vol. 94, no. 1, pp. 42–49, Apr. 1954.

[27] S. Suthram, J. C. Ziegert, T. Nishida, and S. E. Thompson, "Piezoresistance coefficients of (100) silicon nMOSFETs measured at low and high ($\sim$1.5 GPa) channel stress," *IEEE Electron Device Lett.*, vol. 28, no. 1, pp. 58–61, Jan. 2007.

[28] O. Weber, T. Irisawa, T. Numata, M. Harada, N. Taoka, Y. Yamashita, T. Yamamoto, N. Sugiyama, M. Takenaka, and S. Takagi, "Examination of additive mobility enhancements for uniaxial stress combined with biaxially strained Si, biaxially strained SiGe and Ge channel MOSFETs," in *IEDM Tech. Dig.*, 2007, pp. 719–722.

[29] S. E. Thompson, G. Sun, Y. S. Choi, and T. Nishida, "Uniaxial-process-induced strained-Si: Extending the CMOS roadmap," *IEEE Trans. Electron Devices*, vol. 53, no. 5, pp. 1010–1020, May 2006.

[30] A. Dehe, K. Fricke, K. Mutamba, and H. L. Hartnagel, "A piezoresistive GaAs pressure sensor with GaAs/AlGaAs membrane technology," *J. Micromech. Microeng.*, vol. 5, no. 2, pp. 139–142, Jun. 1995.

[31] L. Xia, J. B. Boos, B. R. Bennett, M. G. Ancona, and J. A. del Alamo, "Hole mobility enhancement in $\mathrm{In}_{0.41}\mathrm{Ga}_{0.59}\mathrm{Sb}$ quantum-well field-effect transistors," *Appl. Phys. Lett.*, vol. 98, no. 5, p. 053 505, Jan. 2011.

Ling Xia (S'05) received the B.S. and M.S. degrees in electrical engineering from Peking University, Beijing, China, in 2003 and 2006, respectively. He is currently working toward the Ph.D. degree in the Department of Electrical Engineering and Computer Science, Massachusetts Institute of Technology, Cambridge.

Since 2006, he has been conducting research on III–V p-channel field-effect transistors for logic applications with Microsystems Technology Laboratories, Massachusetts Institute of Technology.

Vadim Tokranov received the M.S. degree in optoelectronic devices with honors from Leningrad Electrical Engineering Institute, St. Petersburg, Russia in 1987 and the Ph.D. degree in physics in 2000 from A. F. Ioffe Physical-Technical Institute, Russian Academy of Science, Saint Petersburg, Russia.

He was a Research Scientist with A. F. Ioffe Physical-Technical Institute from 1987 to 1999. Since 1999, he has been working in the College of Nanoscale Science and Engineering, University at Albany, State University of New York, Albany, NY. He has more than 20 years of experience in design and fabrication and characterization of III–V compound semiconductor devices, including extensive experience in molecular beam epitaxy of quantum-confined heterostructures (As- and Sb-based growth). He has more than 65 papers published in international peer-reviewed journals.

Serge R. Oktyabrsky (SM'08) received the M.S. degree in physics and engineering with honors from Moscow Institute of Physics and Technology, Moscow, Russia, in 1980 and the Ph.D. degree in solid-state physics from Lebedev Physics Institute, Moscow, in 1988.

He is currently a Professor and the Leader of a compound semiconductor team at the College of NanoSciences and NanoEngineering, University at Albany, State University of New York, Albany, NY, specializing in research and development of materials and structures for novel electronic devices. From 1993 to 1998, he was a Visiting Scientist at North Carolina State University, Raleigh, and from 1978 to 1993, he has been with Lebedev Physics Institute as a Senior Scientist and the Head of the electron microscopy group since 1988. He has a more than 30 years of experience in electronic materials, design, fabrication, and characterization of semiconductor electronic and photonic devices and has authored over 200 papers in these fields. His recent research activities focus on physics and technology of quantum-confined structures, microcavity photonic devices, and metal–oxide–semiconductor field-effect transistors based on group III–V.

Dr. Oktyabrsky is a member of The International Society for Optical Engineers, the Materials Research Society, the American Vacuum Society, and the Microscopy Society of America.

Jesús A. del Alamo (F'06) obtained a Telecommunications Engineer degree from the Polytechnic University of Madrid, Madrid, Spain, in 1980 and the M.S. and Ph.D. degrees in electrical engineering from Stanford University, Stanford, CA, in 1983 and 1985, respectively.

From 1985 to 1988, he was with NTT LSI Laboratories, Atsugi, Japan, and since 1988, he has been with the Department of Electrical Engineering and Computer Science, Massachusetts Institute of Technology, Cambridge, where he is currently a Donner Professor and a MacVicar Faculty Fellow. His current research interests are on microelectronics technologies for communications and logic processing. He is also active in online laboratories for science and engineering education.

Prof. del Alamo was a National Science Foundation Presidential Young Investigator. He is a member of the Royal Spanish Academy of Engineering. He currently serves as an Editor of IEEE ELECTRON DEVICE LETTERS.